PICTORIAL ESSAY Oncologic Imaging

^{18}F-NaF PET/CT imaging versus ^{99}mTc-MDP scintigraphy in assessing metastatic bone disease in patients with prostate cancer

Georgios Z. Papadakis, MD, MPH, PhD[1,2], Kostas Marias, PhD[2,3], Corina Millo, MD[4], Apostolos H. Karantanas, MD, PhD[1,2]

[1]*Department of Medical Imaging, Heraklion University Hospital, Medical School, University of Crete, Greece*
[2]*Computational Biomedicine Laboratory (CBML), Institute of Computer Science (ICS), Foundation for Research and Technology Hellas (FORTH), Heraklion, Crete, Greece*
[3]*Technological Educational Institute of Crete, Department of Informatics Engineering, Heraklion, Crete, Greece*
[4]*PET Imaging Center, National Institutes of Health (NIH), Clinical Center (CC), Bethesda, Maryland, USA*

SUBMISSION: 9/4/2019 | ACCEPTANCE: 25/10/2019

ABSTRACT

Prostate Cancer (ProCa) is one of the most commonly encountered malignancies in men, with variable incidence and prevalence rates across different parts of the world. Despite being a slow-growing tumour, ProCa can be fatal when giving distant metastases, with the skeleton being the most common metastatic sites. Osseous metastases in ProCa patients can be osteoblastic, osteolytic or mixed, and are associated with significant morbidity. Thus, early detection and precise assessment of skeletal involvement is critical for prognosis and accurate management of ProCa patients. Conventional bone scintigraphy (BS) using 99m-Technetium (^{99m}Tc) labelled radiopharmaceuticals with planar imaging, SPECT imaging and hybrid SPECT/CT imaging, has been employed for decades in the assessment of metastatic bone disease of ProCa patients, due to its low cost and availability. However, skeletal imaging with modern hybrid PET/CT systems using ^{18}Fluorine-Sodium fluoride (^{18}F-NaF), exhibits superior diagnostic performance compared to conventional BS in addressing the task of evaluating bony involvement in ProCa patients. The superior spatial resolution of PET over SPECT, the preferable pharmacokinetics of ^{18}F-NaF over ^{99m}Tc labelled agents, and the superior inherent quantitative capabilities of PET-imaging, result in the superior diagnostic performance of ^{18}F-NaF PET/CT imaging, which is documented in the current review article. Given the widespread avail-

CORRESPONDING AUTHOR, GUARANTOR

Georgios Z. Papadakis
MD, MPH, PhD, Institute of Computer Science (ICS), Computational Biomedicine Laboratory (CBML), Foundation for Research and Technology Hellas (FORTH), Heraklion, Crete, Greece, 100 N. Plastira, Vassilika Vouton, 70013, Crete, Greece,
E-mail: gzpapadakis@gmail.com

ability of PET/CT scanners, and the decreasing cost of ^{18}F-NaF production, it is recommended that conventional BS should be replaced by the superior ^{18}F-NaF PET/CT imaging in the work-up of ProCa patients.

KEY WORDS

^{18}F-NaF PET/CT imaging, ^{99m}Tc-MDP scintigraphy, Metastatic bone disease, Prostate Cancer

Introduction

Prostate Cancer (ProCa) is the third most commonly diagnosed cancer (7.1% of all cases), after lung cancer, and breast cancer in women, and among the leading causes of cancer-related deaths worldwide (3.8%) [1]. According to recent publications, ProCa has the highest incidence rate among men in 105 countries and the highest mortality rate in 47 countries with about 1.3 million new cases and 359,000 associated deaths in 2018 [1]. The decreasing incidence and mortality trends observed in the last decade have exhibited a tendency to increase, over the last three years [1-3].

Genetic factors, ageing and race are well-established ProCa risk factors [4-5]. Genome-wide association studies (GWAS) have reported at least 100 single-nucleotide polymorphism loci (SNPs) associated with ProCa [5-13]. Family history is positively and significantly correlated with ProCa risk [5, 10-11]. Furthermore, nutrition-related factors have been implied to correlate with increased ProCa risk, such as diets enriched in saturated fat and calcium [14].

Serum prostate-specific antigen (PSA), a glycoprotein produced by the epithelial cells of the prostate gland, is the most commonly used biomarker for ProCa screening [15-16]. The introduction of serum PSA assessment in the 1970s, revolutionised the management of ProCa patients, with increased PSA levels implicating increased risk for ProCa, higher pathological grade and elevated risk for metastatic disease [16]. However, serum PSA assessment lacks specificity, since increased PSA levels can be attributed to several benign conditions such as prostatitis, prostatic hyperplasia, recent medical procedures (biopsy, urinary catheter placement, etc), urinary tract infection, or intense exercise [17]. Furthermore, biopsy-proven ProCa has been confirmed only in 30-40% of cases with increased serum PSA levels (>4 ng/ml), while ProCa has been diagnosed in approximately 15% of men with low serum PSA levels (<4 ng/ml) [17-19]. Therefore, novel fluid-based biomarkers/models are being investigated for ProCa screening, with blood-based Prostate Health Index (PHI) and urine-based Prostate Cancer Antigen 3 (PCA3) having been recently approved by the US Food and Drug Administration (FDA) for ProCa screening [20].

The standard diagnostic algorithm for ProCa diagnosis in patients with elevated serum PSA levels involves prostate sampling with transrectal ultrasound (TRUS)-guided biopsy [21]. Risk stratification based on microscopic architecture and cell appearance in biopsy findings is numerically expressed by the Gleason grading system [22-23]. The TRUS-guided approach has been criticised for the anterior and apical prostate region undersampling, resulting in underdetection of 21% to 28% of malignant cases and in undergrading of 40% of cases, when compared to histology results obtained postoperatively [21-23]. Epstein et al. in a study of patients undergoing radical prostatectomy, reported that the majority of tumours with a Gleason score 2-4 on needle biopsy were upgraded to Gleason score 5-6 when reviewed by pathologists after surgery [24]. Furthermore, since TRUS-guided biopsy is associated with significant morbidity. Multi-Parametric Magnetic Resonance Imaging (MP-MRI) has been suggested as a triage imaging test to guide decision making on which patients with elevated PSA will undergo needle biopsy [25-26]. The MP-MRI images may also be superimposed on TRUS-images during biopsy, with preliminary studies demonstrating that this fusion imaging significantly increases the detection of high-risk tumours as compared to traditional TRUS biopsy [27].

ProCa can give distant metastases to the liver, lymph nodes, lungs, brain and predominately to the bones, with autopsy studies showing skeletal involvement in 90% of patients with advanced metastatic disease [28-30]. ProCa cells spread into the vasculature and preferentially adhere to bone marrow endothelial cells (BMECs). ProCa cell CD44 expression, being associated with hyaluronian binding, facilitates ProCa cells arrest on BMECs and their invasion through the vascular wall into the marrow [31]. Even if ProCa cells have disseminated into the marrow, there may be

a long tumour dormancy period until there is evidence of metastatic disease due to insufficient angiogenesis, immune response, genomic instability and failure to establish a functional stroma [30-32].

Osseous metastases can be complicated with pain, pathologic fractures, hypercalcaemia, bone marrow suppression and spinal cord compression in case of vertebral metastatic lesions extending into the spinal canal [33]. Therefore, early detection of bone metastases in ProCa patients is of utmost importance for the accurate patient management [34-35]. The aim of the current review article is to compare the diagnostic performance of conventional bone scintigraphy (planar, SPECT, or SPECT/CT) using ^{99m}Tc-MDP (^{99m}-Technetium-Methylene Diphosphonate) with hybrid PET/CT imaging using ^{18}Fluorine- Sodium Fluoride (^{18}F-NaF), in assessing bone metastases of ProCa patients.

^{99}mTc-MDP Bone Scintigraphy

^{99m}Tc-MDP whole-body bone scintigraphy (BS) is the most widely employed imaging test for the detection of metastatic bone disease. ^{99m}Tc-MDP is taken up via chemical absorption onto hydroxyapatite crystals on mineralising bone surface and is incorporated into the hydroxyapatite crystalline structure. Therefore, it targets the bone areas with increased osteoblastic activity and active bone metabolism. Especially in the setting of ProCa, skeletal metastatic lesions usually exhibit an abnormally increased osteoblastic activity, making ^{99m}Tc-MDP an effective tracer for visualisation of bone metastases. However, intense osteoblastic activity may occur due to therapy response (flare phaenomenon), various disorders such as trauma, postoperative changes, degenerative changes, and inflammatory/infectious diseases, increasing the number of false positive findings and downgrading the specificity of the technique [36-38]. Furthermore, ^{99m}Tc-MDP lacks efficiency in targeting osteolytic metastatic lesions, which are also encountered in ProCa patients [37].

The National Institute of Health and Clinical Excellence in UK recommends ^{99m}Tc-MDP BS for patients in intermediate or high ProCa risk, indicated by PSA≥10 ng/ml, Gleason Score ≥ 7 or both [39]. Although data on the usefulness of ^{99m}Tc-MDP BS in ProCa staging is controversial, most studies conclude that BS is not recommended for patients with minimal risk for bone metastases (PSA<10 ng/ml). In accordance with the National Institute of Health and Excellence, Briganti et al., suggested that ^{99m}Tc-MDP BS should be performed in patients with a Gleason Score ≥7 or PSA≥10 ng/ml and cT2/T3 disease prior to treatment [39,40]. Ritenour et al., reported that ProCa patients with a Gleason Score >7 and PSA≥10 ng/ml or with a Gleason Score≤7 and PSA≥30 ng/ml should undergo BS [41]. In a retrospective study based on a cohort of 703 newly diagnosed ProCa patients, Lin et al. strongly recommended BS for patients with PSA ≥ 20 ng/ml or Gleason score >7, indicating that BS is of limited value for those with PSA<20 ng/ml and Gleason score<8 [42]. Furthermore, Langsteger et al. reported that, urologists should require BS after radical prostatectomy even if PSA levels are elevated after surgery, due to correlation between the pattern of PSA increasing levels and BS positivity [35].

Even-Sapir et al. reported BS sensitivity, specificity, positive predictive value (PPV), and negative predictive value (NPV) of 70%, 57%, 64%, and 55%, respectively, in a prospective study involving 44 patients with high-risk ProCa, and bone metastases present in 23 of them, based on definitive PET/CT findings, biopsy, and imaging follow-up [43]. In a cohort of 49 ProCa patients with confirmed skeletal involvement in 32 of them, Damle et al., reported sensitivity, specificity, PPV and NPV of 96.9%, 41.2%, 75.6% and 87.5% respectively [44]. Furthermore, Rathke et al., in a study assessing the detection rate of osseous metastases in a cohort of 21 metastatic castrate-resistant prostate cancer (CRPC) patients, reported a sensitivity of 76% (Standard error, SE=3%) and specificity of 90% (SE=2%) [45]. With regard to BS sensitivity in assessing therapy response, there is equivocal data. Treatment response in ProCa patients with known osseous metastases exhibit scintigraphic changes with a delay of 6-8 months. Furthermore, a newly seen lesion on BS bone, within the first six months from the onset of treatment, may indicate healing of a previously occult lesion rather than a new metastasis [36, 46].

In order to enhance the diagnostic performance of BS, Imbriaco et al. introduced the Bone Scintigraphy Index (BSI), in an attempt to create a quantitative and objective tool, that could serve as an imaging biomarker [47]. BSI represents the percentage of the skeleton with neoplastic involvement, and is based on the visual assessment of the extent of the fractional involvement of each bone based on the bone scan. Several studies have reported the prognostic value of BSI for ProCa patient survival. Meirelles et al., in a study including 51 patients with progressing metastatic ProCa, as shown by increasing PSA levels, or by an increase in pre-existing lesions in BS, or by CT or MRI findings, reported that BSI was proved to be a strong prognosticator, with a BSI ≤ 1.27 for a median survival of 27 months and a

BSI>1.27 (P=0.004) for a median survival of 14.4 months [48]. Furthermore, Dennis et al., in a retrospective study involving 88 CRPC patients, reported that a doubling in BSI is associated with a 1.9-fold increase in the risk of death [49]. In the same context, Reza et al. reported that the 5-year survival rate of patients following androgen deprivation therapy (ADT) is significantly different between patients with BSI ≤1 and BSI >1 [50].

However, BSI is based on visual interpretation of scans and requires considerable time from the reader. Therefore, computer-assisted diagnosis (CAD) and artificial intelligence were developed and employed for automated BSI assessment. Zaccho et al. reported that BSI, assessed via automated software, is an independent risk factor for the time from androgen deprivation therapy (ADT) initiation to development of resistance to castration (CR) in hormone-naïve, newly diagnosed, patients [51]. In the study which included 208 men undergoing ADT therapy, BSI significantly (p<0.001) predicted the time to CR development with a hazard ratio of 1.17 [51]. In a similar study by Poulsen et al., software-based assessment of BSI was statistical significantly predicting the time to CR-development (hazard ratio [HR] 1.45; C-index increase from 0.49 to 0.69) and the ProCa-specific survival (PCSS) (HR 1.34; C-index increase from 0.76 to 0.95) [52]. Armstrong et al., in a multicenter randomised, double-blinded, placebo-controlled clinical trial, including 1245 patients with bone metastatic chemotherapy-naïve CR-ProCa from 241 sites in 37 countries, reported that the risk of death increases by 20% per automated BSI doubling (HR, 1.20; p<0.001) [53]. They also reported that overall survival (OS) for a BSI of 0.05 was 34.7 months, for a BSI of 0.58 was 27.3 months, for BSI of 2.06 was 21.7 months and for BSI of 6.72 was 13.3 months. Automated BSI was also found to be associated with PCSS (HR, 1.20; p<0.001), time to symptomatic progression (HR, 1.18; p<0.001), and time to opiate use for cancer pain (HR, 1.21; p<0.001) [53]. Furthermore, a meta-analysis by Li et al., including 14 studies with 1295 metastatic ProCa patients in total (12 of them using automated BSI), showed that increased baseline BSI and BSI change during treatment significantly predict poor OS (HR=1.29, P < 0.001; HR=1.27, P< 0.001, respectively). In addition, baseline BSI was significantly associated with ProCa-specific survival (HR=1.65, P=0.019) and prostate specific antigen recurrence survival (HR=2.26, P< 0.001) [54].

Spatial information in the 3D image space, and therefore, accurate anatomic characterisation of metastatic bone lesions is limited in planar BS due to the 2D nature of acquisition. This inherent drawback is a major obstacle, when evaluating skeletal regions such as the spine, pelvis, hip, knee, small bones and joins where bone structures overlap on the 2D images. In order to overpass the aforementioned diagnostic challenge, BS with single photon emission computed tomography (SPECT) was introduced, enabling image reconstruction in 3D space. Performing BS with SPECT acquisition increases the diagnostic performance and improves the accuracy of the test [43]. Moreover, hybrid SPECT/CT imaging, provides incremental diagnostic information, by allowing anatomic characterisation of regions with abnormally increased ^{99m}Tc-MDP uptake. The capability of SPECT/CT to depict lesion morphology contributes significantly to addressing the task of differentiating malignant from benign lesions [43, 55-62]. In a prospective comparison between whole-body planar scintigraphy (WBS), SPECT, and SPECT/CT in 353 oncologic patients, the reported sensitivity, specificity, NPV and PPV on a per-patient basis were 93%, 78%, 95% and 59% for WBS, 94%, 71%, 97% and 53 % for SPECT, and 97 %, 94 %, 97 % and 88 % for SPECT/CT, respectively. The presented data clearly showed the significantly improved specificity and PPV provided by SPECT/CT scintigraphy, which enabled accurate downstaging and upstaging of disease status, significantly affecting patient management [63].

Even-Sapir et al., in a cohort of 44 ProCa patients, evaluating the impact of BS with SPECT acquisition in terms of diagnostic performance, found that sensitivity, specificity, PPV and NPV were increased by 21%, 10%, 13% and 19% respectively when assessing skeletal metastatic spread [43]. In a prospective comparison study between planar BS and SPECT/CT BS in 37 newly diagnosed ProCa patients with PSA≥50 ng/ml, Fonager et al. demonstrated that SPECT/CT BS outperformed planar BS in all diagnostic properties [64]. Furthermore, Sharma et al., in a study of 99 ProCa patients showed that BS with SPECT/CT correctly characterised 96% of equivocal lesions observed in planar BS [65]. Also, Helyar et al. compared the diagnostic performance of SPECT/CT BS over planar BS and SPECT BS in a cohort of 40 ProCa patients and found that 61% of lesions were rated as equivocal in planar BS and SPECT BS, whereas only 8% of lesions were deemed equivocal with SPECT/CT BS [58]. Additionally, Palmedo et al., in a cohort of 97 ProCa patients showed that SPECT/CT BS significantly influenced patient management, by downstaging metastatic disease in 33.8% of patients [63]. In the same context a retrospective study by Fleury et al. including 164 ProCa patients, showed that trunk SPETC/CT

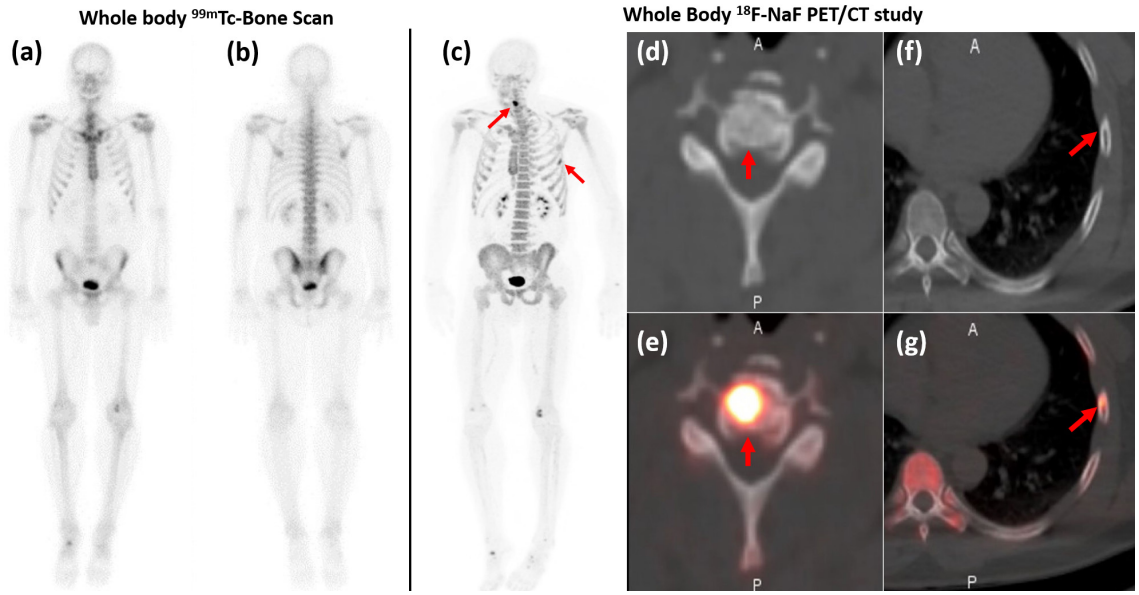

Fig. 1. *A 56-year-old man with newly diagnosed ProCa, (PSA 2910 ng/mL), who underwent both conventional whole-body bone scan with ^{99m}Tc-MDP, and whole-body PET/CT with ^{18}F-NaF (20 days interval between the two tests) for staging purposes.* ***a, b.*** *Anterior and posterior views of whole-body ^{99m}Tc-Bone Scan were negative for bone metastases.* ***c.*** *Whole-body maximum intensity projection (MIP) ^{18}F-NaF PET image showing (arrows) focal ^{18}F-NaF avid lesions located in the cervical spine and in lateral left 6th rib.* ***d, e.*** *Axial CT and ^{18}F-NaF PE/CT images of the cervical spine showing intensely increased ^{18}F-NaF uptake, corresponding to an osteosclerotic lesion at the C5 vertebral body, strongly indicating an osseous metastatic lesion.* ***f, g.*** *Axial CT and ^{18}F-NaF PE/CT images of the thorax, showing abnormally increased ^{18}F-NaF activity at the lateral left 6th rib, corresponding to a hardly seen on CT osteosclerotic lesion, highlighting the capability of the modality to target early-stage metastatic bone lesions. (Image courtesy of Dr. P. Choyke, Molecular Imaging Program Director, National Cancer Institute, Bethesda, MD, USA).*

provides incremental diagnostic information over planar BS, contributing to the assessment of metastatic bone disease with significantly improved accuracy [66] .

^{18}F-NaF PET/CT imaging

Fluorine-18 Sodium Fluoride (^{18}F-NaF) has been introduced in NM as a radiotracer for bone imaging since 1962 and was FDA approved in 1972 [67, 68]. Being a positron emitter, its high energy photons (511keV), its short half-life ($T_{1/2}$ = 110 minutes), and limitations in detector imaging technology at that period, did not favour the clinical use of ^{18}F-NaF for skeletal imaging. On the contrary, bone scintigraphy with ^{99m}Tc-MDP, which was easily accessible due to the greater availability of molybdenum generators, evolved as the most widely employed NM imaging technique for bone imaging. The favourable physical characteristics of ^{99m}Tc- for planar BS and SPECT, mainly due to emission of lower energy photons, and the limited availability of clinical PET scanners initially, led to the establishment of ^{99m}Tc-MDP as the most widely employed radiotracer for visualisation of skeletal metastases. However, the widespread installation of clinical PET and PET/CT systems, enabled the clinical implementation of ^{18}F-NaF as bone-seeking radiopharmaceutical for functional skeletal imaging [69-81]. The favourable ^{18}F-NaF pharmacokinetics and the superior inherent quantitative and diagnostic capabilities provided by hybrid PET/CT systems compared to conventional BS, renewed the interest for ^{18}F-NaF PET/CT as the optimal imaging modality for evaluation the osseous metastases [69].

The mechanism of ^{18}F-NaF uptake by bone is similar to that of ^{99m}Tc-MDP. However, ^{18}F-NaF presents superior kinetics, such as faster blood clearance and twofold higher uptake by bone compared to ^{99m}Tc-MDP [37]. Post intravenous injection, ^{18}F- ions reach rapidly an equilibrium with plasma, and most of the radiotracer is captured by bone in a single pass of blood, through fluorine and hydroxyl ions exchange on the surface of hydroxyapatite crystals, forming fluoroapatite [34]. Compared to ^{99m}Tc-MDP, ^{18}F-NaF exhibits minimal binding to serum proteins, resulting in fast clearance from soft tissues, shorter delay times from injection

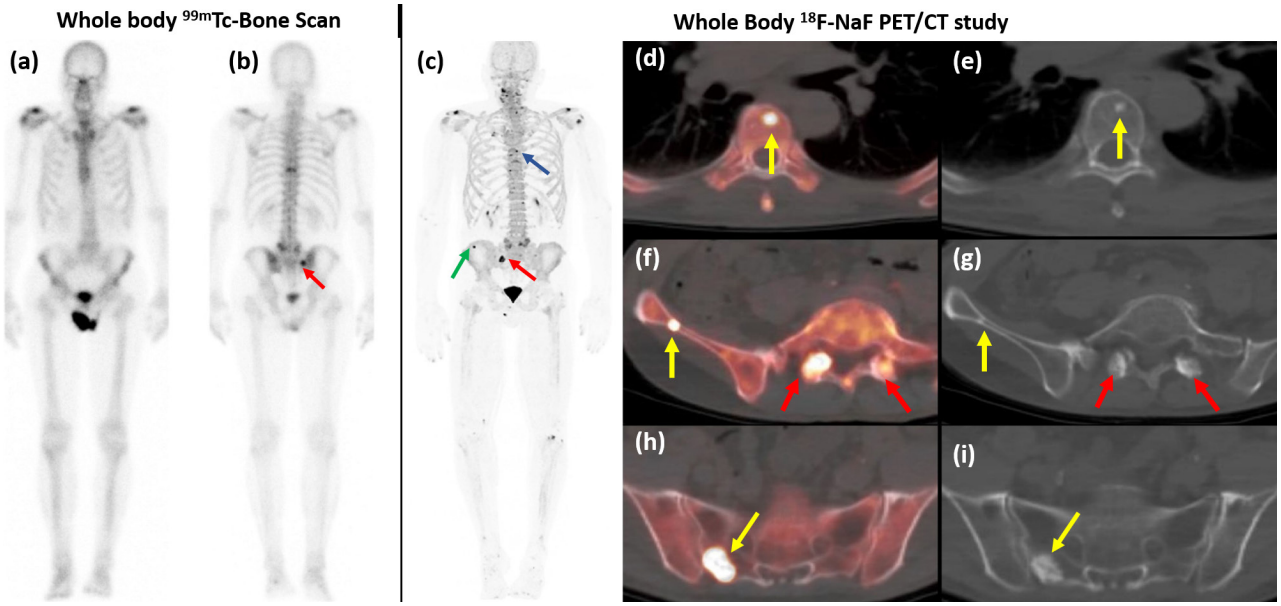

Fig. 2. *A patient with prostatic adenocarcinoma post prostatectomy (Gleason 4+3=7 positive margins, both seminal vesicle (SV) positive for invasion, T3bN0Mx). The patient underwent salvage radiation, plus therapy with luteinising hormone-releasing hormone agonists for six months, with PSA being undetectable for two years. Subsequently, an increase in PSA levels was observed and the patient underwent both conventional whole-body bone scan with ^{99m}Tc-MDP, and whole-body PET/CT with ^{18}F-NaF within follow-up (14 days interval between the two scans).* ***a, b.*** *Anterior and posterior views of whole-body ^{99m}Tc-Bone Scan revealed a metastatic lesion at the right sacrum (arrow).* ***c.*** *Whole-body maximum intensity projection ^{18}F-NaF PET image showing foci of abnormally elevated ^{18}F-NaF activity at the right sacrum (red arrow), and additional lesions at a thoracic vertebra (blue arrow) and at the right iliac wing (green arrow).* ***d, e.*** *Axial CT and ^{18}F-NaF PE/CT images of the thoracic spine showing intensely increased ^{18}F-NaF uptake, corresponding to an osteosclerotic lesion at the body of the T5 vertebra (arrows).* ***f, g.*** *Axial CT and ^{18}F-NaF PE/CT images of the pelvis, showing abnormally increased ^{18}F-NaF activity at the right iliac wing (yellow arrows), co-localising with an osteosclerotic focus on CT. Areas with elevated ^{18}F-NaF activity seen on the facet joints L5-S1 (red arrows) correspond to degenerative changes seen on CT (osteophytes).* ***h, i.*** *Axial CT and ^{18}F-NaF PE/CT images of the pelvis showing abnormally increased ^{18}F-NaF activity at the right sacrum, corresponding to an area of osteosclerosis on CT, consistent with metastatic lesion. (Image courtesy of Dr. P. Choyke, Molecular Imaging Program Director, National Cancer Institute, Bethesda, MD, USA).*

to image acquisition, and shorter imaging times increasing thus patient comfort [35, 37, 69].

^{18}F-NaF PET/CT demonstrates considerable advantages over BS, mainly due to ^{18}F-NaF pharmacokinetic properties and the better imaging characteristics of PET compared to SPECT. In terms of diagnostic quality of the acquired images, the higher ^{18}F-NaF bone to soft tissue ratio uptake, contributes to reduced image noise and increased sensitivity **(Figs. 1 and 2)**. Due to this high ^{18}F-NaF bone to background ratio uptake, it has been suggested, yet not been applied and confirmed in a diagnostic environment, that CT scan may not be needed for attenuation correction and should be performed only for co-registration purposes [82].

Furthermore, the ability of ^{18}F-NaF to target bone disorders leading to increased bone surface exposed to blood flow, enables visualisation of both osteoblastic and osteolytic bone, metastases, whereas conventional BS depicts only osteoblastic lesions [35,67]. Moreover, the quantitative capabilities of PET-imaging allow to follow up the activity of each individual lesion [SUV (standardised uptake value)-based metrics] [83], while providing skeletal tumour burden indices of total ^{18}F-NaF skeletal metastatic lesion uptake and total volume of ^{18}F-NaF positive bone metastases, with critical contribution to accurate assessment of treatment response **(Fig. 3, 4)** [79, 80]. In a study by Muzahir et al., SUV_{max} for skeletal metastases on CR-ProCa patients was found to be significantly higher compared to degenerative lesions (SUV_{max}>50 for met-

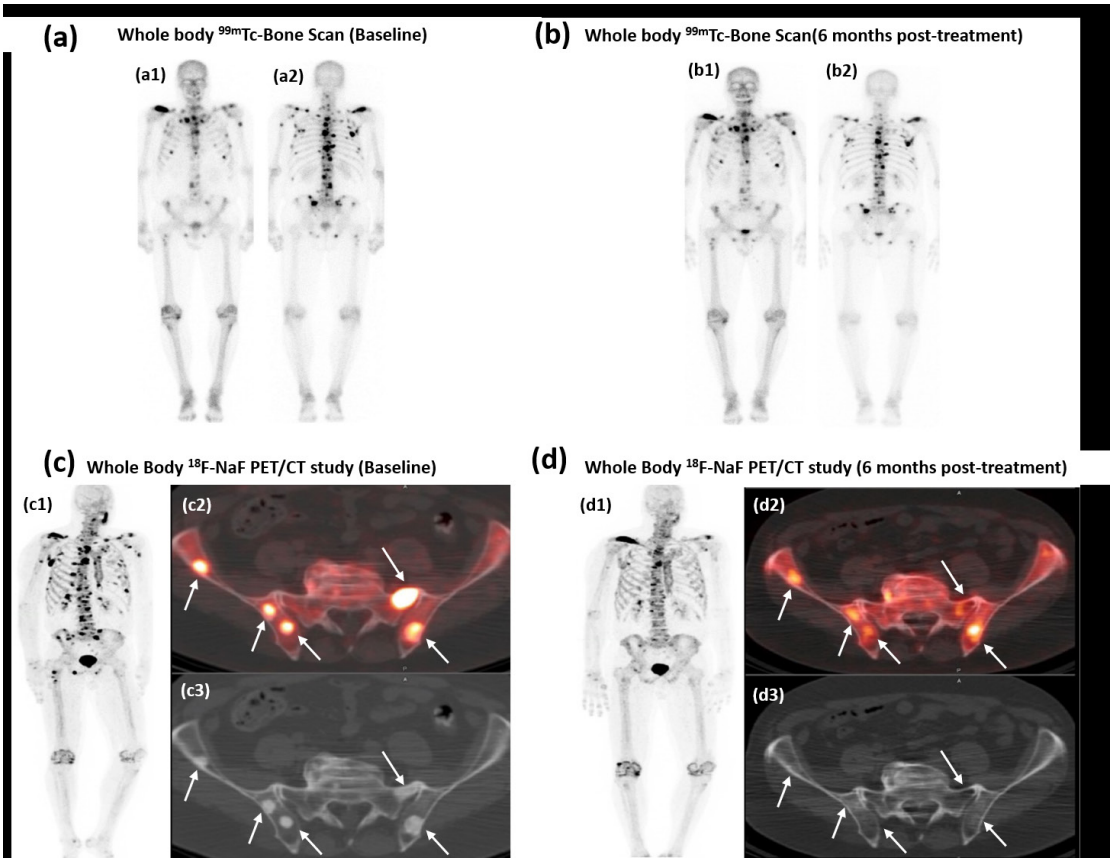

Fig. 3. *A case of a 62-year-old man with history of ProCa who was evaluated with both whole-body ^{99m}Tc-MDP bone scan and whole-body ^{18}F-NaF PET/CT study, before initiation of therapy and six months after therapy completion, in order to assess treatment response. (^{99m}Tc-MDP bone scan and ^{18}F-NaF PET/CT scan were performed with one day interval from each other, at both time points).* ***a.*** *Anterior (a1) and posterior (a2) view of whole-body ^{99m}Tc-Bone Scan showing extensive skeletal involvement.* ***b.*** *Anterior (b1) and posterior (b2) view of whole-body ^{99m}Tc-Bone Scan 6 months post treatment indicates stable metastatic bone disease.* ***c.*** *Baseline whole-body ^{18}F-NaF PET/CT study revealing more osseous metastatic sites, seen on the MIP image (c1). The ^{18}F-NaF PET/CT study performed six months post treatment* ***(d)*** *showed improvement with decreased ^{18}F-NaF activity for the majority of skeletal lesions. The osteosclerotic appearance on the CT portion of the study was almost resolved for several bone metastases (comparison between subfigures: c3 and d3). (Image courtesy of Dr. P. Choyke, Molecular Imaging Program Director, National Cancer Institute, Bethesda, MD, USA).*

astatic disease, < 12 for degenerative lesions) (P< 0.001) [84].

Simoncic et al. compared ^{18}F-NaF and ^{18}F-FDG(radiolabeled glucose analog reflecting tumour metabolism) for the assessment of pharmacodynamic response to therapy in 10 CR-ProCa patients with osseous metastases, with scans obtained prior to therapy, after 4 weeks of therapy, and post 2 weeks of treatment cessation [85]. Authors suggested that ^{18}F-NaF and ^{18}F-FDG-based response assessment is comparable, yet the use of both tracers could be proved beneficial. Nowadays, that theranostics (use of identical or similar agents for both imaging and treatment) lie on the basis of precision medicine, ^{18}F-NaF PET/CT can be a significant tool for the implementation of such models in visualising and treating osseous metastases of ProCa patients. In a recent review by Jadvar et al., pre-treatment total ^{18}F-NaF positive bone metastases correlate with patient outcome, when applying alpha particle therapy with $^{223}RaCl_2$ (approved by FDA on 2013). Moreover, ^{18}F-NaF contributes to the assessment of response to $^{223}RaCl_2$, given that the ^{18}F-NaF PET/CT scan is performed sufficiently long after the end of the treatment (2-3 months) in order to avoid the flare period, which can mimic disease progression [86]. Zukotynski et al. also described the superiorty of ^{18}F-NaF PET/CT over conventional

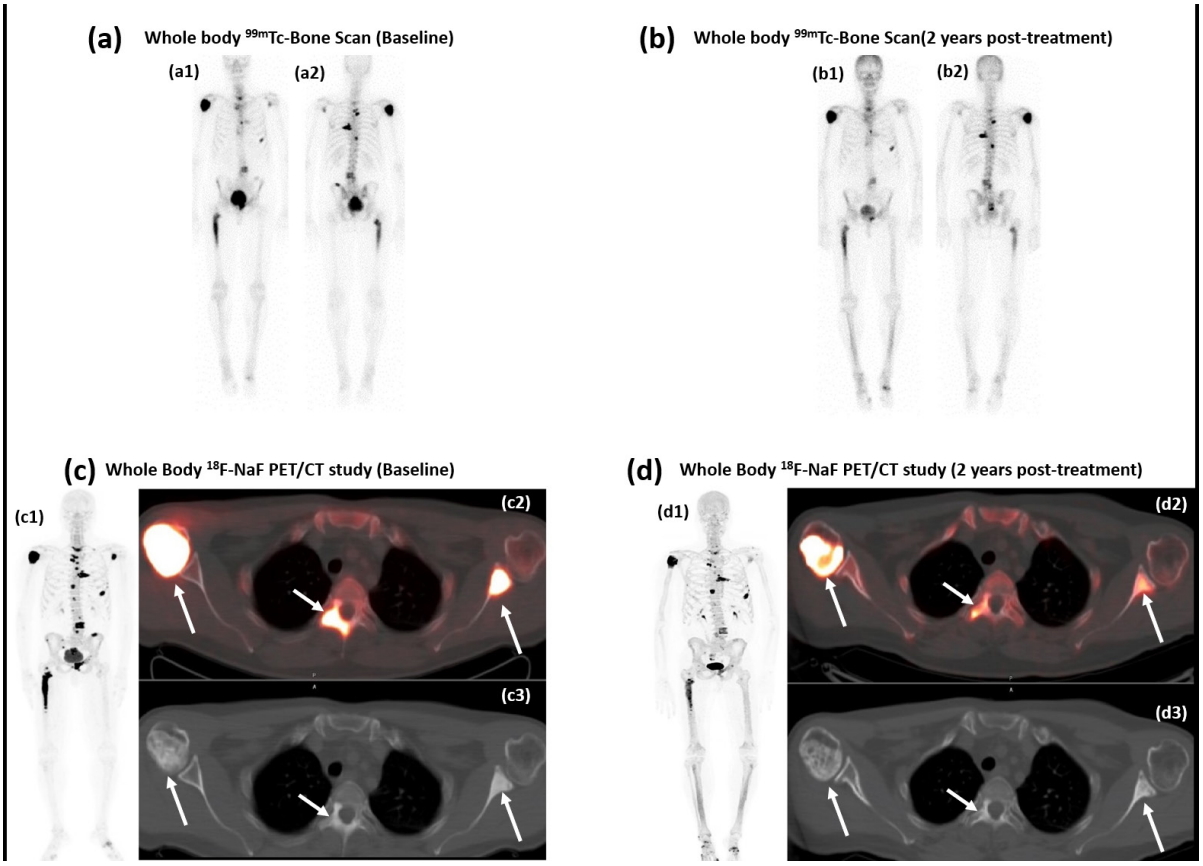

Fig. 4. *A case of a 62-year-old man with history of ProCa who was evaluated with both whole-body ^{99m}Tc-MDP bone scan and whole-body ^{18}F-NaF PET/CT study, before initiation of therapy and two years after therapy completion, in order to assess treatment response. (^{99m}Tc-MDP bone scan and ^{18}F-NaF PET/CT scan were performed with one day interval from each other, at both time points).* ***a.*** *Anterior (a1) and posterior (a2) view of whole-body ^{99m}Tc-Bone Scan revealed several sites of bony involvement.* ***b.*** *Anterior (b1) and posterior (b2) view of whole-body ^{99m}Tc-Bone Scan, two years post treatment, showed the same osseous metastatic sites without significant change, indicating stable metastatic skeletal disease.* ***c.*** *Baseline whole-body ^{18}F-NaF PET/CT study demonstrated additional skeletal metastases, seen on the MIP image (c1). Moreover, the ^{18}F-NaF PET/CT study performed two years post treatment* ***(d)*** *showed improvement in terms of both decreased ^{18}F-NaF uptake, and CT appearance of the lesions. (Image courtesy of Dr. P. Choyke, Molecular Imaging Program Director, National Cancer Institute, Bethesda, MD, USA).*

BS in assessing treatment response in the setting of CR-ProCa patients [87]. Furthermore, Apolo et al. reported prognostic value of ^{18}F-NaF PET/CT with significant correlation between OS with both SUV change at 6 months (P=0.018) and number of lesions on the baseline scan (P=0.017) [88].

Dose-wise, due to rapid renal excretion of fluorine ions, urinary bladder is the organ which receives the highest dose in ^{18}F-NaF PET/CT, compared to bone surface in ^{99m}Tc-MDP BS. The radiation-induced risk of a ^{18}F-NaF PET exam has been reported to be about 4.4-8.9 mSv, with an additional 2.0-4.0 mSv for the CT acquisition, while the effective dose of a ^{99m}Tc-MDP scan is 4.2-6.3 mSv. However, time-of-flight PET and the high target-to-background signal of ^{18}F-NaF, which allow lower administered activities without influencing the diagnostic outcome, and low dose CT acquisitions, obtained with dose reduction techniques such as tube current modulation, adaptive collimation and iterative reconstruction algorithms, may reduce the radiation dose of ^{18}F-NaF PET/CT exams [37].

Comparison between ^{18}F-NaF PET/CT and ^{99m}Tc-MDP scintigraphy in the assessment of metastatic skeletal disease in ProCa patients

PubMed data base search resulted in six prospective studies (table 1). Poulsen et al. compared the diagnostic accuracy of ^{18}F-NaF PET/CT, ^{18}F-fluoromethylcholine (^{18}F-FCH) PET/

Table 1. Studies comparing ^{18}F-NaF PET/CT imaging and ^{99}mTc-MDP scintigraphy in assessing skeletal metastases in patients with prostate cancer.

Study	Number of patients	^{18}F -NaF				^{99}mTc-MDP planar BS				Other			
		^{1}SN (%)	^{1}SP (%)	^{1}PPV (%)	^{1}NPV (%)	^{1}SN (%)	^{1}SP (%)	^{1}PPV (%)	^{1}NPV (%)	^{1}SN (%)	^{1}SP (%)	^{1}PPV (%)	^{1}NPV (%)
Poulsen et al[77], *	50	93.1	54.0	81.8	77.9	50.8	82.2	86.4	42.9	^{2}84.7	^{2}91.1	^{2}95.0	^{2}74.9
Even-Sapir et al[43], *	44	100	100	100	100	57.0	57.0	59.0	55.0	^{3}92.0	^{3}82.0	^{3}87.0	^{3}100
Iagaru et al[79], *	18	100	80.0			87.5	80			^{4}55.6	^{4}100		
Minamimoto et al [80],*	15	^{5}100	^{5}60.0	^{5}94.1	^{5}100	81.3	100	100	45.5	^{6}65.4	^{6}40.0	^{6}85.0	^{6}25.0
Jambor et al[81], *	27	^{7}94	^{7}96			^{7}54	^{7}88			^{8}81	^{8}96		
Fonager et al[57], *	37	89	90	96	75	78	90	96	60	^{8}89	^{8}100	^{8}100	^{8}77

*1. SN: sensitivity, SP: specificity, PPV: positive predictive value, NPV: negative predictive value, 2. Results obtained from ^{18}F-FCH PET/CT, 3. Results obtained from SPECT, 4. Results obtained from ^{18}F-FDG PET/CT, 5. Results obtained from combined ^{18}F-NaF / ^{18}F-FDG scan, 6. Results obtained from whole-body MRI, 7. Results correspond to diagnostic performance for assessing osseous metastases in both breast and ProCa patients, 8. Results obtained from SPECT/CT, *prospective study*

CT, and ^{99m}Tc-MDP BS, in detecting spinal metastasis in a prospective study of 50 biopsy-proven ProCa patients, using magnetic resonance imaging (MRI) as a reference [89]. ^{18}F-fluoromethylcholine (^{18}F-FCH) is a choline analogue, a precursor of phospholipids incorporated into phosphatidylcholine, and is a potential marker of cell division via tracing choline kinase which is overexpressed in tumour cells [90]. The mean age of the enrolled patients was 73 years, with 363 malignant and 163 non-malignant lesions. The study found superior diagnostic performance of PET/CT using both ^{18}F-NaF and ^{18}F-FCH over ^{99m}Tc-MDP BS. The reported values for sensitivity, specificity, PPV and NPV values were 51, 82, 86, 43% respectively for whole body BS, and 93, 54, 82, 78% respectively for ^{18}F-NaF PET/CT.

Even-Sapir et al., compared the performance of ^{99m}Tc-MDP planar BS, single- and multiple field-of-view SPECT, ^{18}F-NaF PET and ^{18}F-NaF PET/CT in detecting bone metastases in a prospective series of 44 high risk ProCa patient with a total of 156 lesions (mean age, 71.6±8.8 years) [43]. Authors reported sensitivity, specificity, PPV and NPV values of 57, 57, 59, 55% respectively for ^{99m}Tc-MDP BS, 92%, 82%, 86%, 90% respectively for SPECT, 100%, 82%, 87%, 100% respectively for ^{18}F-NaF PET and, 100%, 82%, 87%, 100% respectively for ^{18}F-NaF PET/CT. The study revealed the superior performance of ^{18}F-NaF PET compared to ^{99m}Tc-MDP BS either planar or SPECT, while the fused CT images in ^{18}F-NaF PET/CT significantly increased the specificity.

Iagaru et al. conducted a prospective evaluation of ^{99m}Tc-MDP, ^{18}F-NaF PET/CT and ^{18}F-FDG PET/CT for detection of skeletal metastases in a cohort of 18 ProCa patients. The study showed that ^{18}F-NaF PET/CT outperformed both ^{99m}Tc-MDP and ^{18}F-FDG PET/CT in sensitivity (100% vs 87.5% and 55.6% respectively) [91]. Furthermore, in a prospective cohort of 15 ProCa patients, Minamimoto et al compared the performance of combined administration of ^{18}F-NaF and ^{18}F-FDG in a single PET/CT scan with ^{99m}Tc-MDP BS and with whole-body MRI, which included both unenhanced and contrast-enhanced sequences. ^{18}F-NaF/^{18}F-FDG PET/CT exhibited considerably higher sensitivity than whole-body MRI (P<0.02) and BS (P<0.03) in the assessment of skeletal lesions. However, ^{18}F-NaF/^{18}F-FDG PET/CT did not show any significant difference in sensitivity with a combination of whole-body MRI and BS (P=0.08), or with a combination of ^{18}F-NaF/^{18}F-FDG PET/CT and whole-body MRI (P=1.00). Despite the small size of the study population, this data suggests that combined ^{18}F-NaF/^{18}F-FDG PET/CT is superior to

whole-body MRI and ^{99m}Tc-MDP scintigraphy as single imaging modalities, for the assessment of skeletal involvement in ProCa patients [92].

Jambor et al. compared the diagnostic accuracy of ^{99m}Tc-hydroxymethane diphosphonate (^{99m}Tc-HDP) planar BS, ^{99m}Tc-HDP SPECT, ^{99m}Tc-HDP SPECT/CT, ^{18}F-NaF PET/CT and whole-body MRI, including diffusion weighted imaging, (DWI-wbMRI) for the detection of bone metastases in a prospective series of 27 ProCa patients at high risk for skeletal involvement [93]. On a lesion-based analysis, the study demonstrated that ^{18}F-NaF PET/CT and DWI-wbMRI exhibited significantly higher sensitivity and AUC values compared to conventional nuclear medicine imaging tests. Fonager et al. compared planar BS, SPECT/CT and ^{18}F-NaF PET/CT in detecting skeletal metastases in a prospective cohort of 37 newly diagnosed ProCa patients with PSA≥50, eligible for ADT therapy, with skeletal involvement being present in 27 of them [64]. The study showed that both ^{18}F-NaF PET/CT and SPECT/CT outperformed planar BS in terms of sensitivity (89% for both ^{18}F-NaF PET/CT and SPECT/CT versus 78% for planar BS). Although, the study did not reveal any significant differences regarding specificity, authors recommended the incorporation of ^{18}F-NaF PET/CT in the work-up of ProCa patients.

Conclusions and future perspectives

Early and accurate assessment of metastatic bone disease in ProCa patients is critical for prognosis and efficient patient management, with significant implications in health care costs. ^{18}F-NaF PET/CT is the hybrid imaging modality of choice for targeting and characterising both benign and malignant bone processes, leading to increased bone surface exposed to blood flow. In the setting of ProCa patients, literature data presented in the current review article, strongly support the superior diagnostic performance of ^{18}F-NaF PET/CT over conventional BS in terms of increased specificity and lower rate of false positive findings, in the evaluation of metastatic skeletal disease. Given the increasing availability of clinical PET/CT scanners, the decreasing cost of PET-radiopharmaceuticals' production, and the substantial morbidity which is associated with metastatic bone disease, ^{18}F-NaF PET/CT is evolving as the new imaging standard of reference for ProCa patients, at risk for skeletal involvement.

^{18}F-FDG is more effective in targeting osteolytic and early-stage bone marrow metastases before leading to osseous reaction, providing complementary information to ^{18}F-NaF, when assessing the skeletal involvement in ProCa patients. Furthermore, ProCa-specific tissue markers such as prostate specific membrane antigen (PSMA), can be effectively targeted with PMSA-ligands radiolabelled with various positron emitting isotopes such as gallium-68 (^{68}Ga), fluorine-18 (^{18}F), or copper-64 (^{64}Cu), holding promise for enhanced applications of PET-imaging in assessing metastatic bone disease in the setting of ProCa patients [94, 95]. **R**

Conflict of interest

The authors declared no conflicts of interest.

References

1. Bray F, Ferlay J, Soerjomataram I, et al. Global cancer statistics 2018: GLOBOSCAN estimates of incidence and mortality worldwide for 36 cancers in 185 countries. *CA Cancer J Clin* 2018; 68: 394-424.
2. Cronin KA, Lake AJ, Scott S, et al. Annual report to the nation on the status of cancer, Part II: National cancer statistics. *Cancer* 2018; 124(13): 2785-2800.
3. Negoita S, Feuer EJ, Mariotto A, et al. Annual report to the nation on the status of cancer, Part II: Recent changes in prostate cancer trends and disease characteristics. *Cancer* 2018; 124(13): 2801-2814.
4. Taitt HE. Global trends and prostate cancer: a review of incidence, detection, and mortality as influenced by race, ethnicity, and geographic location. *Am J Mens Health* 2018; 12(6): 1807-1823.
5. Attard G, Parker C, Edes RA et al. Prostate Cancer. *Lancet* 2016; 387: 70-82.
6. Ewing CM, Ray AM, Lange EM, et al. Germline mutations in HOXB13 and prostate-cancer risk. *N Engl J Med* 2012; 366: 141-149.
7. Breast cancer linkage consortium. Cancer risks in BRCA2 mutation carriers. J *Natl Cancer Inst* 1999; 91: 1310-1316.
8. Kote-Jarai Z, Leongamornlert D, Saunders E, et al. BRCA2 is a moderate penetrance gene contributing to young-onset prostate cancer: implications for ge-

netic testing in prostate cancer patients. *Br J Cancer* 2011; 105: 1230-1234.
9. Chen H, Ewing CM, Zheng S, et al. Genetic factors influencing prostate cancer in Norwegian men. *Prostate* 2018; 78(3): 186-192.
10. Perez-Cornago A, Key TJ, Allen NE, et al. Prospective investigation of risk factors for prostate cancer in the UK Biobank cohort study. *Br J Cancer* 2017; 117(10): 1562-1571.
11. Bostwick DG, Burke HB, Djakiew D, et al. Human prostate cancer risk factors. *Cancer* 2004; 101(10 Suppl): 2371-490.
12. American Cancer Society. Cancer facts & figures for African Americans 2016-2018. Atlanta: *American Cancer Society*, 2016.
13. Layne TM, Graubard BI, Ma X, et al. Prostate cancer risk factors in black and white men in the NIH-AARPdiet and health study. *Prostate Cancer Prostatic Dis* 2019; 22(1): 91-100.
14. Gathirua-Mwangi WG, Zhang J. Dietary factors and risk of advanced prostate cancer. *Eur J Cancer Prev* 2014; 23(2): 96-109.
15. Pezaro C, Woo HH, Davis ID. Prostate cancer: measuring PSA. *Intern Med J* 2014; 44(5): 433-440.
16. Hatakeyama S, Yoneyama S, Tobisawa Y, et al. Recent progress and perspectives on prostate cancer biomarkers. *Int J Clin Oncol* 2017; 22: 214-221.
17. Saini S. PSA and beyond: alternative prostate cancer biomarkers. *Cell Oncol (Dordr)* 2016; 39(2): 97-106.
18. Leal J, Welton NJ, Martin RM, et al. Estimating the sensitivity of a prostate cancer screening programme for different PSA cut-off levels: A UK case study. *Cancer Epidemiol* 2018; 52: 99-105.
19. Koie T, Mitsuzuka K, Narita S, et al. A solitary positive prostate cancer biopsy does not predict a unilateral lesion in radical prostatectomy specimens. *Scand J Urol* 2015, 49(2): 103-107.
20. Hendriks RJ, van Oort IM, Schalken JA. Blood-based and urinary biomarkers: a review and comparison of novel biomarkers for detection and treatment decisions. *Prostate Cancer Prostatic Dis* 2017; 20(1): 12-19.
21. Verma S, Choyke PL, Eberhardt SC, et al. The current state of MR Imaging - targeted biopsy techniques for detection of prostate cancer. *Radiology* 2017; 285 (2): 343-356.
22. Litwin MS, Tan HJ. The diagnosis and treatment of prostate cancer. *JAMA* 2017; 317(24): 2532-2542.
23. Epstein JI, Amin MB, Reuter VE, et al. Contemporary Gleason grading of prostatic carcinoma. An update with discussion on practical issues to implement the 2014 international society of urological pathology (isup) consensus conference on Gleason grading of prostatic carcinoma. *Am J Surg Pathol* 2017; 41(4): e1-e7.
24. Epstein JI. Gleason score 2-4 adenocarcinoma of the prostate on needle biopsy. *Am J Surg Pathol* 2000; 24(4): 477-478.
25. Caverly TJ, Hayward RA, Reamer E et al. Presentation of benefits and harms in US cancer screening and prevention guidelines: systematic review. *J Natl Cancer Inst* 2016; 108: djv436.
26. Ahmed HU, El-Shater Bosaily A, Brown LC, et al. Diagnostic accuracy of multiparametric MRI and TRUS biopsy in prostate cancer (PROMIS): a paired validating confirmatory study. *Lancet* 2017; 389 (10071): 815-822.
27. Siddiqui MM, Rais-Bahrami S, Turkbey B, et al. Comparison of MR/Ultrasound fusion-guided biopsy with ultrasound-guided biopsy for the diagnosis of prostate cancer. *JAMA* 2015; 313(4): 390-397.
28. Bitting RL, Schaeffer D, Somarelli JA et al. The role of epithelial plasticity in prostate cancer dissemination and treatment resistance. *Cancer Metastasis Rev* 2014; 33(2-3): 441-468.
29. Jin J-K, Dayyani F, Gallick GE. Steps in prostate progression that lead to bone metastasis. *Int J Cancer* 2011; 128: 2545-2561.
30. Gartrell BA and Saad F. Managing bone metastases and reducing skeletal related events in prostate cancer. *Nat Rev Clin Oncol* 2014; 11(6): 335-345.
31. Morrissey C and Vessella RI. The role of tumor microenvironment in prostate cancer bone metastasis. *J Cell Biochem* 2007; 101(4): 873-86.
32. Van der Toom E, Verdone JE, Pienta KJ. Disseminated tumor cells and dormancy in prostate cancer metastasis. *Curr Opin Biotechnol* 2016; 40: 9-15.
33. Rubens RD. Bone metastases: incidence and complications. In: Mundy GR, Rubens RD. *Cancer and the skeleton*. London, England: Martin Dunitz, 2000; 33-42.
34. Ozulker T, Uzun AK, Ozulker F, et al. Comparison of ^{18}F-FDG-PET/CT with ^{99m}Tc-MDP bone scintigraphy for the detection of bone metastases in cancer patients. *Nucl Med Commun* 2010; 31(6): 597-603.
35. Langsteger W, Rezaee A, Pirich C, et al. ^{18}F-NaF-PET/

CT and ^{99m}Tc-MDP Bone scintigraphy in the detection of bone metastases in prostate cancer. *Semin Nucl Med* 2016; 46(6): 491-501.

36. Messiou C, Cook G, de Souza NM. Imaging metastatic bone disease from carcinoma of the prostate. *Br J Cancer* 2009; 101(8): 1225-1232.
37. Mick CG, James T, Hill DJ et al. Molecular imaging in oncology: ^{18}F-Sodium Fluoride PET imaging of osseous metastatic disease. *AJR Am J Roentgenol* 2014; 203(2): 263-271.
38. Kanishi D. 99mTc-MDP accumulation mechanisms in bone. *Oral Surg Oral Med Oral Pathol* 1993;75(2):239-246.
39. National institute for clinical excellence: Improving outcomes in urological cancer (2002). https://www.nice.org.uk/guidance/ csg2 Accessed 19 Jul 2016.
40. Briganti A, Passoni N, Ferrari M, et al. When to perform bone scan in patients with newly diagnosed prostate cancer: external validation of the currently available guidelines and proposal of a novel risk stratification tool. *Eur Urol* 2010; 57(4): 551-558.
41. Ritenour CW, Abbott JT, Goodman M, et al. The utilization of Gleason grade as the primary criterion for ordering nuclear bone scan in newly diagnosed prostate cancer patients. *ScientificWorldJournal* 2009; 9: 1040-1045.
42. Lin Y, Mao Q, Chen B, et al. When to perform scintigraphy in patients with newly diagnosed prostate cancer? A retrospective study. *BMC Urol* 2017; 17(1): 41.
43. Even-Sapir E, Metser U, Mishani E, et al. The detection of bone metastases in patients with high-risk prostate cancer: ^{99m}Tc-MDP planar bone scintigraphy, single- and multi-field-of-view SPECT, ^{18}F-fluoride PET, and ^{18}F-Fluoride PET/CT. *J Nucl Med* 2006; 47(2): 287-297.
44. Damle NA, Bal C, Bandopadhyaya GP, et al. The role of ^{18}F-fluoride PET-CT in the detection of bone metastases in patients with breast, lung and prostate carcinoma: a comparison with ^{18}F-FDG PET/CT and ^{99m}Tc-MDP bone scan. *Jpn J Radiol* 2013; 31(4): 262-269.
45. Rathke H, Afshar-Oromieh A, Giesel FL, et al. Intraindividual comparison of ^{99m}Tc-Methylene Diphosphonate and prostate-specific membrane antigen ligand ^{99m}Tc-MIP-1427 in patients with osseous metastasized prostate cancer. *J Nucl Med* 2018; 59(9): 1373-1379.
46. Ciray I, Astrom G, Andreasson I, et al. Evaluation of new sclerotic bone metastases in breast cancer patients during treatment. *Acta Rad* 2000; 41(2): 178-182.
47. Imbriaco M, Larson SM, Yeung HW, et al. A new parameter for measuring metastatic bone involvement by prostate cancer: The bone scan index. *Clin Cancer Res* 1998; 4:1765-1772.
48. Meirelles GSP, Schroder H, Ravizzini, et al. Prognostic value of baseline [^{18}F] Fluorodeoxyglucose positron emission tomography and ^{99m}Tc-MDP bone scan in progressing metastatic prostate cancer. *Clin Cancer Res* 2010; 16(24): 6093-6099.
49. Dennis ER, Jia X, Mezheritskiy IS, et al. Bone scan index: a quantitative treatment response biomarker for castration resistant metastatic prostate cancer. *J Clin Oncol* 2012; 30(5): 519-524.
50. Reza M, Bjartell A, Ohlsson M, et al: Bone scan index as a prognostic imaging biomarker during androgen deprivation therapy. *EJNMMI Res* 2014; 4:58.
51. Zacho HD, Gade M, Mortensen JC, et al. Bone Scan Index is an independent predictor of time to castration-resistant prostate cancer in newly diagnosed prostate cancer: A prospective study. *Urology* 2017; 108: 135-141.
52. Poulsen MH, Rasmussen J, Edenbrandt, L et al. Bone scan index predicts outcome in patients with metastatic hormone-sensitive prostate cancer. *BJU* Int 2016; 117(5): 748-753.
53. Armstrong AJ, Anand A, Edenbrandt L, et al. Phase 3 assessment of the automated bone scan index as a prognostic imaging biomarker of overall survival in men with metastatic castration-resistant prostate cancer. A secondary analysis of a randomized clinical trial. *JAMA Oncol.* 2018; 4(7): 944-951.
54. Li D, Lv H, Hao X, et al. Prognostic value of bone scan index as imaging biomarker in metastatic prostate cancer: a meta-analysis. *Oncotarget* 2017; 8(48): 84449-84458.
55. Shen G, Deng H, Jia Z. Comparison of choline-PET/CT, MRI, SPECT, and bone scintigraphy in the diagnosis of bone metastasis in patients with prostate cancer: a meta-analysis. *Skeletal Radiol* 2014; 43: 1503-1513.
56. O'Sullivan GJ, Carty FL, Cronin CG. Imaging of bone metastasis: an update. *World J Radiol* 2015; 28; 7(8): 202-211.
57. Römer W, Nömayr A, Uder M, Bautz W, Kuwert T. SPECT-guided CT for evaluating foci of increased bone metabolism classified as indeterminate on

SPECT in cancer patients. *J Nucl Med* 2006; 47: 1102-1106.
58. Helyar V, Mohan HK, Barwick T, et al. The added value of multislice SPECT/CT in patients with equivocal bony metastasis from carcinoma of the prostate. *Eur J Nucl Med Mol Imaging* 2010; 37: 706-713.
59. Ndlovu X, George R, Ellmann A, et al. Should SPECT-CT replace SPECT for the evaluation of equivocal bone scan lesions in patients with underlying malignancies? *Nucl Med Commun* 2010; 31: 659-665.
60. Zhang Y, Shi H, Gu Y, et al. Differential diagnostic value of single-photon emission computed tomography/spiral computed tomography with Tc-99m-methylene diphosphonate in patients with spinal lesions. *Nucl Med Commun* 2011; 32: 1194-1200.
61. Jiang L, Han L, Tan H, et al. Diagnostic value of 99mTc-MDP SPECT/spiral CT in assessing indeterminate spinal solitary lesion of patients without malignant history. *Ann Nucl Med* 2013; 27: 460-467.
62. Cook GJ, Azad G, Padhani AR. Bone imaging in prostate cancer: the evolving roles of nuclear medicine and radiology. *Clin Transl Imaging* 2016; 4: 439-447.
63. Palmedo H, Marx C, Ebert A, et al. Whole-body SPECT/CT for bone scintigraphy: diagnostic value and effect on patient management in oncological patients. *Eur J Nucl Med Mol Imaging*. 2014; 41(1): 59-67.
64. Fonager RF, Zacho HD, Langkilde NC, et al. Diagnostic test accuracy of ^{18}F-sodium fluoride PET/CT, ^{99m}TC - labelled diphosphonate SPECT/CT, and planar bone scintigraphy for diagnosis of bone metastases in newly diagnosed, high-risk prostate cancer. *Am J Nucl Med Mol Imaging* 2017; 7(5): 218-227.
65. Sharma P, Dhull VS, Reddy RM, et al. Hybrid SPECT-CT for characterizing isolated vertebral lesions observed by bone scintigraphy: Comparison with planar scintigraphy, SPECT, and CT. *Diagn Interv Radiol* 2013; 19: 33-40.
66. Fleury V, Ferrer L, Colombié M, et al. Advantages of systematic trunk SPECT/CT to planar bone scan (PBS) in more than 300 patients with breast or prostate cancer. *Oncotarget* 2018 3; 9(60): 31744-31752.
67. Araz M, Aras G, Kucuk ON. The role of ^{18}F-NaF PET/CT in metastatic bone disease. *J Bone Oncol* 2015; 4: 92-97.
68. Blau M, Nagler W, Bender MA. Fluorine-18: a new isotope for bone scanning. *J Nucl Med* 1962; 3: 332-334.
69. Bastawrous S, Bhargava P, Behnia F, et al. Newer PET application with an old tracer: role of ^{18}F-NaF skeletal PET/CT in oncologic practice. *Radiographics.* 2014; 34(5): 1295-316.
70. Papadakis GZ, Manikis GC, Karantanas AH, et al. 18F-NaF uptake by fibrous dysplasia bone lesions is positively associated with bone turnover markers (BTMs). *Eur J Nucl Med Mol Imaging* 2019; 45(Suppl 1): S241-S241.
71. Papadakis GZ, Manikis GC, Karantanas AH, et al. Prognostic utility of 18F-NaF PET/CT imaging for fractures in patients with fibrous dysplasia of bone. *Eur J Nucl Med Mol Imaging* 2019; 45(Suppl 1): S241-S242.
72. Papadakis G, Manikis G, Karantanas A, et al. Fibrous dysplasia related 18F-NaF activity in the spine is significantly higher in patients with scoliosis, compared to patients without spinal deformity. *J Nucl Med* 2019; 60 (suppl 1): 1298-1298.
73. Papadakis G, Manikis G, Karantanas A, et al. Positive association between fibrous dysplasia (FD) related 18F-NaF activity and bone turnover markers (BTMs). *J Nucl Med* 2019; 60 (suppl 1): 90-90.
74. Hartley I, McCarthy T, Papadakis G, et al. Treatment of Gorham-Stout Disease with Combination Sirolimus and Denosumab. *J Endocr Soc* 2019; 3 (suppl 1): MON-517.
75. Papadakis GZ, Jha S, Karantanas AH, et al. Prospective evaluation of the application of ^{18}F-NaF PET/CT imaging in melorheostosis *Eur J Nucl Med Mol Imaging* 2018; 45(Suppl 1): S231-S232.
76. Papadakis GZ, Jha S, Bhattacharyya T, et al. ^{18}F-NaF PET/CT in extensive melorheostosis of the axial and appendicular skeleton with soft-tissue involvement. *Clin Nucl Med* 2017; 42(7): 537-539.
77. Papadakis GZ, Millo C, Bagci U, et al. ^{18}F-NaF and ^{18}F-FDG PET/CT in Gorham-Stout Disease. *Clin Nucl Med* 2016; 41(11): 884-885.

78. Papadakis GZ, Millo C, Bagci U, et al. Value of ^{18}F-NaF PET/CT imaging in the assessment of Gorham-Stout disease activity. *Eur J Nucl Med Mol Imaging* 2016; 43(suppl 1): S597-S597.
79. Papadakis GZ, Manikis GC, Karantanas AH, et al. Application of ^{18}F-NaF PET/CT imaging in fibrous dysplasia. *Horm Res Paediatr* 2017; 88 (suppl 1): 20-20.
80. Papadakis G, Manikis G, Karantanas A, et al. Application of ^{18}F-NaF PET/CT imaging in prognosis of fractures and treatment planning in patients with fibrous dysplasia. *J Nucl Med* 2017; 58 (suppl 1): 308-308.
81. Papadakis GZ, Manikis GC, Karantanas AH, et al. ^{18}F-NaF PET/CT imaging in fibrous dysplasia of bone. *J Bone Miner Res* 2019; 34(9): 1619-1631.
82. Segall G, Delbeke D, Stabin MG, et al. SNM practice guideline for sodium ^{18}F-fluoride PET/CT bone scans 1.0. *J Nucl Med* 2010; 51(11): 1813-20.
83. Vali R, Beheshti M, Waldenberger P, et al. Assessment of malignant and benign bone lesions by static ^{18}F-Fluoride PET-CT: Additional value of SUV!. *J Nucl Med* 2008; 49: 150 (suppl 1).
84. Muzahir S, Jeraj R, Liu G, et al. Differentiation of metastatic vs degenerative joint disease using semi-quantitative analysis with ^{18}F-NaF PET/CT in castrate resistant prostate cancer patients. *Am J Nucl Med Mol Imaging* 2015; 5: 162-168.
85. Simoncic U, Perlman S, Liu G, et al. Comparison of NaF and FDG PET/CT for assessment of treatment response in castrate-resistant prostate cancers with osseous metastases. *Clin Genitourin Cancer* 2015; 13(1): e7-e17.
86. Jadvar H, Colletti PM. ^{18}F-NaF/^{223}RaCl2 theranostics in metastatic prostate cancer: treatment response assessment and prediction of outcome. *Br J Radiol.* 2018; 91(1091): 20170948.
87. Zukotynski KA, KimCK, Gerbaudo VH, et al. ^{18}F-FDG-PET/CT and ^{18}F-NaF-PET/CT in men with castrate-resistant prostate cancer. *Am J Nucl Med Mol Imaging* 2015; 5: 72-82.
88. Apolo AB, Lindenberg L, Shih JH, et al. Prospective study evaluating ^{18}F-NaF-positron emission tomography/computed tomography (^{18}F-NaF-PET/CT) in predicting clinical outcomes and survival in advanced prostate cancer. *J Nucl Med.* 2016; 57(6): 886-892.
89. Poulsen MH, Petersen H, Hoilund-Carlsen PF, et al. Spine metastases in prostate cancer: Comparison of technetium-99m-MDP whole - body bone scintigraphy, [^{18}F] choline positron emission tomography (PET)/computed tomography (CT) and [^{18}F] NaF PET/CT. *BJU Int* 2014; 114: 818-823.
90. Vali R, Loidl W, Pirich C, et al. Imaging of prostate cancer with PET/CT using ^{18}F-Fluorocholine. *Am J Nucl Med Mol Imaging* 2015; 5(2): 96-108.
91. Iagaru A, Mittra E, Dick DW, et al. Prospective evaluation of ^{99m}Tc MDP scintigraphy, ^{18}F NaF PET/CT, and ^{18}F FDG PET/CT for detection of skeletal metastases. *Mol Imaging Biol* 2012; 14: 252-259.
92. Minamimoto R, Loening A, Jamali M, et al. Prospective Comparison of ^{99m}Tc-MDP Scintigraphy, Combined ^{18}F-NaF and ^{18}F-FDG PET/CT, and whole-body MRI in patients with breast and prostate cancer. *J Nucl Med* 2015; 56(12): 1862-1868.
93. Jambor I, Kuisma A, Ramadan S, et al. Prospective evaluation of planar bone scintigraphy, SPECT, SPECT/CT, ^{18}F-NaF PET/CT and whole body 1.5T MRI, including DWI, for the detection of bone metastases in high risk breast and prostate cancer patients: SKELETA clinical trial. *Acta Oncol* 2016; 55(1): 59-67.
94. Ceci F, Castellucci P, Fanti S. Current application and future perspectives of prostate specific membrane antigen PET imaging in prostate cancer. *Q J Nucl Med Mol Imaging* 2019; 63(1): 7-18.
95. Treglia G, Pereira Mestre R, Ferrari M, et al. Radiolabelled choline versus PSMA PET/CT in prostate cancer restaging: a meta-analysis. *Am J Nucl Med Mol Imaging* 2019; 9(2): 127-139.

READY - MADE CITATION

Papadakis GZ, Marias K, Millo C, Karantanas AH. ^{18}F-NaF PET/CT imaging versus ^{99}mTc-MDP scintigraphy in assessing metastatic bone disease in patients with prostate cancer. *Hell J Radiol 2019*; 4(4): 42-55.